Hindawi
Journal of Applied Mathematics
Volume 2023, Article ID 9920157, 9 pages
https://doi.org/10.1155/2023/9920157

Research Article

Theoretical Error Analysis of Hybrid Finite Difference–Asymptotic Interpolation Method for Non-Newtonian Fluid Flow

Shafaruniza Mahadi,[1] **Su Hoe Yeak**,[2] **Norazam Arbin**,[1] **and Faisal Salah**[3]

[1]*Mathematical Sciences Studies, College of Computing, Informatics and Media, Universiti Teknologi MARA Johor Branch, Segamat Campus, 85000 Segamat, Johor Darul Takzim, Malaysia*
[2]*Department of Mathematical Sciences, Faculty of Science, Universiti Teknologi Malaysia, 81310 Johor Bahru, Johor, Malaysia*
[3]*Department of Mathematics, College of Science and Arts, King Abdul-Aziz University, Rabigh, Saudi Arabia*

Correspondence should be addressed to Shafaruniza Mahadi; shafa669@uitm.edu.my

Received 29 September 2022; Revised 26 January 2023; Accepted 21 February 2023; Published 9 March 2023

Academic Editor: Waqar A. Khan

In this paper, we utilized a hybrid method for the unsteady flow of the non-Newtonian third-grade fluid that combines the finite difference with the asymptotic interpolation method. This hybrid method is used to satisfy the semiunbound domain condition of the fluid flow's length approaching infinity. The primary issue with this research is how much of the hybrid approach's error may be accepted to guarantee that the method is significant. This paper discussed theoretical error analysis for numerical solutions, including the range and norm of error. The perturbation method's concept is used to assess the hybrid method's error. It is discovered that the hybrid approach's relative error norm is lower than that of the finite difference method. In terms of the error standard, the hybrid approach is more consistent. Error analysis is performed to check for the accuracy as well as the platform for variable mesh size finite difference method in the future research.

1. Introduction

Non-Newtonian fluid flow has always been in the limelight due to the difficulty of the equation. Physical behaviors and properties of fluid make researchers believe that there is no equation with a complete problem variable exist in one equation. Non-Newtonian fluid problem appears such as in designing body vest for police [1] and landslides [2]. Differential types, rate type, and integral type are three types of fluid models in non-Newtonian fluid [3–5]. The derivatives of the local deformation tensor with respect to time determine the type of differential. Materials with limited memory, such as diluted polymeric solutions, are described using a rate type model. High-memory materials, such as polymeric melts, are regarded as integral types. Second, third, and fourth grades are the three subclasses that make up differential type. The most basic non-Newtonian fluid subclass, known as second-grade fluid, can only describe typical stress differences. On the other hand, the governing equations for third- and fourth-grade fluids are substantially more complicated, and these fluids can indicate shear thickening (viscosity increases with higher stress) or thin (viscosity reduces with increased stress).

This present paper focused on differential type of third-grade fluid. Blood is believed to be a third-grade magnetohydrodynamics (MHD) fluid while the arteries are porous [6]. Besides, the applications of non-Newtonian fluid can be seen in the industrial manufacturing process such as production of magnetic materials, polymer technology, and metallurgy [7, 8].

The third-grade fluid problem can be seen in Hayat et al. [9], where the MHD fluid that flows between two porous plates has been solved using a perturbation method to produce an exact solution. Abelman et al. [10] investigated the third-grade MHD fluid with rotation of the z-axis and the fluid filling the porous half-place. The boundary condition (BC) of the problem included a semi-infinite domain; thus, the BC is converted to a finite domain. The same procedure has been applied in Hayat and Wang [11] and later is solved numerically using the MATLAB programming.

The unsteady constants and variables of the accelerated third-grade MHD are investigated using the homotopy

analysis method (HAM) [12]. For every fluid problem, HAM required a different convergence property and only accurate between finite interval [0, 1] domain as proved by Van and Robert [13]. Ghani et al. [14] explored an incompressible third-grade MHD fluid in a unidirectional thin film flow over an oscillating inclined belt embedded in a porous medium using the ideal homotopy asymptotic method and the homotopy pertubation method.

Technique of perturbation has been practised to solve MHD free convection from vertical porous plate with a diffusion-thermo effect [15]. However, according to Şenol et al. [16], perturbation methods have a narrow range of validity and valid for weakly nonlinear problems.

Laplace transform has been used to solve accelerated free convection rotating flows of second-grade fluid [17]. However, this analytical method needs more time especially for large problem system.

Rawi et al. [18] and Gaffar et al. [19] applied Keller-box method in solving convective boundary layer flow of micropolar Jeffery fluid with prescribed wall temperature and thermal convection of an incompressible non-Newtonian fluid from a horizontal circular cylinder. Nevertheless, this method needs high computational work at each time step [20].

The fluid problem which involved infinite condition can be found in Rahman et al. [21]. In this research, thermal radiation and nonuniform heat sources or sinks are taken into account together with a hybrid nanofluid flow of heat transmission towards an extending surface. Through similarity transformations, the governing partial differential equations generated from the Navier-Stokes equations are transformed into nonlinear ordinary differential equations. The boundary-value problem solver (bvp4c) in the MATLAB package is then used to numerically resolve the model of coupled nonlinear equations.

The FDM is the earliest technique for creating a rectangular grid using space and time coordinates, and it may be used to gauge how accurate a model is. This approach works well for solving partial differential equations (PDEs), which might have variable boundary conditions, be linear or nonlinear, dependant or time-dependent, etc (BCs). The development of high-speed computers with vast amounts of storage has led to the appearance of numerous numerical solution approaches for PDEs. The FDM is still a useful method for resolving these issues, nevertheless, due to its simplicity of usage.

Goud et al. [22] examined for heat radiation in the MHD flow of a micropolar fluid across a moving vertical porous plate. The equations are converted to nondimensional, and the finite difference technique is implemented. In another study, implicit finite difference method and damped Newton method were used to solve the problem of the unsteady third-grade MHD heat transfer with viscous dissipation [23].

In order to estimate an unknown value when a problem's sample size approaches infinity, one can utilize the asymptotic interpolation method (AIM). With enough parameters, the asymptotic functions used in this method can accurately reflect a problem's behavior. The advantage of AIM is highly accurate approximations are obtained in only a few iterations [24].

The third grade of fluid flow in rotating frame as shown in Figure 1 has been addressed by using homotopy analysis method [25]. After all, there is no exact solution that has been produced to this fluid problem.

The combination of the FDM and AIM may solve various models of nonlinear PDEs with an unbounded domain and produce an accurate result in perspective of the strengths of both techniques. Thereby, this current work presents a hybrid finite difference–asymptotic interpolation method to respond to its infinite boundary condition. This hybrid method has been applied in Mahadi et al. [26–28]. The advantage of this hybrid method is the numerical solution obtained will be close to its exact solution. This hybrid method is suitable for the problem related to an infinite domain. This present paper highlights the differential types of third grade which fluid has a derivative of the tensor with respect to time. The aim of this paper is to present an error analysis of the hybrid finite difference and the asymptotic interpolation method.

First, the mathematical formulation is presented. The nonlinear equation is discretize using the finite difference method. Later, the nonlinear least square technique is applied in the asymptotic interpolation method using a special function to find the solution when the problem tends to infinity. Next, an error analysis is conducted. The truncation error is evaluated in the finite difference system. Besides that, the modified fluid problem which has an exact solution is imposed, and the same hybrid algorithm is applied. The results of the error analysis included an absolute error and a relative error.

2. Mathematical Formulation

2.1. Governing Equations. An incompressible third-grade fluid in the space such as in Figure 1, $z > 0$, is considered. The plate at $z = 0$ is moved with a constant acceleration A in the x-direction for $t > 0$ and induced in the motion in the fluid. The fluid and plate are both in the solid body rotation. Initially, they are all at rest. The momentum equations for such problem of the flow following Aziz et al. [25] are

$$\begin{aligned} \operatorname{div} \mathbf{V} &= 0, \\ \rho\left[\frac{\partial \mathbf{V}}{\partial t} + 2\Omega \times \mathbf{V} + \Omega \times (\Omega \times r)\right] &= -\nabla p + \operatorname{div} \mathbf{T}, \end{aligned} \tag{1}$$

where ρ is the density of fluid and $\mathbf{V}$ is the velocity of fluid relative to the rotating frame; meanwhile, $\partial \mathbf{V}/\partial t$ is rate of change of $\mathbf{V}$ in the frame. Ω is the angular velocity where it represents the axis of which fluid is rotating. The product of $2\Omega \times \mathbf{V}$ is a Cariolis acceleration. It presents the fluid is flowing relative to the rotating coordinate system. r is the radial coordinate with $r^2 = x^2 + y^2$. $\Omega \times (\Omega \times r)$ is centripetal acceleration (direction of the change in velocity towards the center), and p is the pressure [12, 25]. $\mathbf{T}$ is the extra stress tensor with

$$\mathbf{T} = -p\mathbf{I} + \sum_{j=1}^{n} \mathbf{S}_j. \tag{2}$$

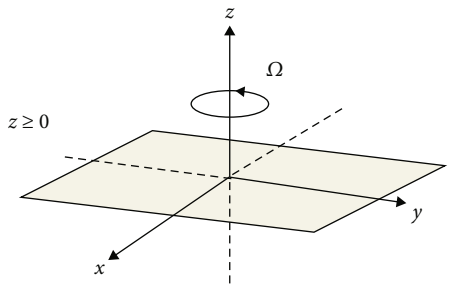

Figure 1: Graphical representation of fluid flow.

The tensors $\mathbf{S}_j$ are given by

$$\begin{aligned}\mathbf{S}_1 &= \mu A_1,\\ \mathbf{S}_2 &= \alpha_1 A_2 + \alpha_2 A_1^2,\\ \mathbf{S}_3 &= \beta_1 A_3 + \beta_2 (A_2 A_1 + A_1 A_2) + \beta_3 \left(tr A_1^2\right) A_1,\end{aligned} \tag{3}$$

where μ is the coefficient of shear viscosity and α and β are the material constants [14, 19]. The constitutive equation of the third-grade fluid is

$$\mathbf{T} = -p\mathbf{I} + \left[\mu + \beta_3 \left(tr A_1^2\right)\right] A_1 + \alpha_1 A_2 + \alpha_2 A_1^2 \tag{4}$$

[9, 23, 25, 29], where A_1 and A_2 are the kinematic tensors [30] such that

$$\begin{aligned}A_1 &= \text{grad } \mathbf{V} + (\text{grad } \mathbf{V})^T = \begin{bmatrix} 0 & 0 & \dfrac{\partial u}{\partial v} \\ 0 & 0 & \dfrac{\partial v}{\partial z} \\ \dfrac{\partial u}{\partial v} & \dfrac{\partial v}{\partial z} & 0 \end{bmatrix},\\ A_2 &= \frac{dA_1}{dt} + A_1(\text{grad } \mathbf{V}) + (\text{grad } \mathbf{V})^T A_1\\ &= \begin{bmatrix} 2\left(\dfrac{\partial u}{\partial z}\right)^2 & 2\left(\dfrac{\partial u \partial v}{\partial z^2}\right) & \dfrac{\partial^2 u}{\partial z \partial t} \\ 2\left(\dfrac{\partial u \partial v}{\partial z^2}\right) & 2\left(\dfrac{\partial v}{\partial z}\right)^2 & \dfrac{\partial^2 v}{\partial z \partial t} \\ \dfrac{\partial^2 u}{\partial z \partial t} & \dfrac{\partial^2 v}{\partial z \partial t} & 0 \end{bmatrix}.\end{aligned} \tag{5}$$

From (1),

$$\begin{aligned}2\Omega \times \mathbf{V} &= 2\Omega \times \begin{vmatrix} i & j & k \\ u & v & 0 \end{vmatrix} = 2\Omega u - 2\Omega v,\\ \Omega \times (\Omega \times r) &= \Omega \times \begin{vmatrix} i & j \\ \Omega & \Omega \\ x & y \end{vmatrix} = -\Omega^2 x - \Omega^2 y.\end{aligned} \tag{6}$$

Next, substitute (6) into (1); the equation can be written in the matrix form

$$\rho \begin{bmatrix} \dfrac{\partial u}{\partial t} - 2v\Omega - x\Omega^2 \\ \dfrac{\partial v}{\partial t} - 2u\Omega - y\Omega^2 \\ 0 \end{bmatrix} = -\begin{bmatrix} \dfrac{\partial p}{\partial x} \\ \dfrac{\partial p}{\partial y} \\ \dfrac{\partial p}{\partial z} \end{bmatrix} + \begin{bmatrix} \dfrac{\partial T_{xx}}{\partial x} + \dfrac{\partial T_{xy}}{\partial y} + \dfrac{\partial T_{xz}}{\partial z} \\ \dfrac{\partial T_{yx}}{\partial x} + \dfrac{\partial T_{yy}}{\partial y} + \dfrac{\partial T_{yz}}{\partial z} \\ \dfrac{\partial T_{zx}}{\partial x} + \dfrac{\partial T_{zy}}{\partial y} + \dfrac{\partial T_{zz}}{\partial z} \end{bmatrix}, \tag{7}$$

where T_{xx}, T_{yy}, and T_{zz} are normal stress tensor and T_{xy}, T_{xz}, T_{yx}, T_{yz}, T_{zx}, and T_{zy} are shear stress tensors. Substitute (5) into (4); thus, Equation (7) which represents the third-grade non-Newtonian fluid in a rotating frame [25] is given as follows.

$$\begin{aligned}\frac{\partial f}{\partial \tau} + 2i\Omega_1 f &= \frac{\partial^2 f}{\partial \eta^2} + a\frac{\partial^3 f}{\partial \eta^2 \partial \tau}\\ &\quad + 2b\left[2\left(\frac{\partial^2 f}{\partial \eta^2}\right)\left(\frac{\partial f}{\partial \eta}\right)\left(\frac{\partial \bar{f}}{\partial \eta}\right) + \left(\frac{\partial f}{\partial \eta}\right)^2\left(\frac{\partial^2 \bar{f}}{\partial \eta^2}\right)\right],\end{aligned} \tag{8}$$

where $a = \alpha_1/\rho(A^2/\nu^4)^{1/3}$ and $b = \beta_3/\rho(A^4/\nu^5)^{1/3}$. $f = u + iv$ and $\bar{f} = u - iv$ are the complex functions which involve real and imaginary part of the velocity profile. The boundary conditions are connected to the constant acceleration:

$$\begin{aligned}f(\eta, 0) &= 0,\\ f(0, \tau) &= \tau,\\ f(\eta, \tau) &\longrightarrow 0, \quad \text{as } \eta \longrightarrow \infty.\end{aligned} \tag{9}$$

2.2. Hybrid Finite Difference–Asymptotic Interpolation Method. The fluid problem in (8) poses a nonlinear equation, and thus, the forward and central finite differences are applied to discretize the system with $O(\Delta\eta)$ and $O(\Delta\eta^2)$, respectively. Initially, the problem followed the initial condition as shown in (9). As $\tau = 2$, the forward difference is applied. Then, (8) is

$$\begin{aligned}\frac{f_i^{n+1} - f_i^n}{\Delta\tau} + 2i\Omega_1 f_i^n &= \frac{f_{i+1}^n - 2f_i^n + f_{i-1}^n}{\Delta\eta^2}\\ &\quad + \frac{a}{\Delta\eta^2 \Delta\tau}\left[\left(f_{i+1}^{n+1} - 2f_i^{n+1} + f_{i-1}^{n+1}\right) - \left(f_{i+1}^n - 2f_i^n + f_{i-1}^n\right)\right]\\ &\quad + \frac{b}{\Delta\eta^4}\left(f_{i+1}^n - 2f_i^n + f_{i-1}^n\right)\left(f_{i+1}^n + f_{i-1}^n\right)\left(\bar{f}_{i+1}^n + \bar{f}_{i-1}^n\right)\\ &\quad + \frac{b}{2\Delta\eta^4}\left(f_{i+1}^n + f_{i-1}^n\right)^2\left(\bar{f}_{i+1}^n - 2\bar{f}_i^n + \bar{f}_{i-1}^n\right).\end{aligned} \tag{10}$$

At the period from $\tau > 2$ until $\tau = \tau_{\max} - 1$, the central finite difference is applied, and the equation is shown as

Table 1: Real part of velocity profile at $L = 6,12,18$.

η	$L = 6$	$L = 12$	$L = 18$
0	1	1	1
1	0.3449	0.3449	0.3449
2	0.1163	0.1164	0.1164
3	0.0393	0.03934	0.03934
4	0.0132	0.01337	0.01337
5	0.0040	0.004572	0.004572
6	0	0.001572	0.001572
7	—	0.0005436	0.0005436
8	—	0.000189	0.000189
9	—	0.00006593	0.00006607
10	—	0.00002284	0.00002321
11	—	0.000007159	0.000008194
12	—	0	0.000002905
13	—	—	0.000001034
14	—	—	0.0000003696
15	—	—	0.0000001323
16	—	—	0.0000000469
17	—	—	0.00000001496
18	—	—	0

Table 2: Imaginary part of velocity profile at $L = 6,12,18$.

η	$L = 6$	$L = 12$	$L = 18$
0	0	0	0
1	-0.033190	-0.033190	-0.033190
2	-0.022500	-0.02253	-0.02584
3	-0.011380	-0.01144	-0.01144
4	-0.005033	-0.005175	-0.005175
5	-0.001842	-0.002204	-0.002204
6	0	-0.000904	-0.000904
7	—	-0.0003618	-0.0003618
8	—	-0.0001423	-0.0001424
9	—	-0.00005514	-0.00005531
10	—	-0.00002084	-0.00002128
11	—	-0.000006963	-0.000008131
12	—	0	-0.000003089
13	—	—	-0.000001168
14	—	—	-0.0000004397
15	—	—	-0.0000001648
16	—	—	-0.00000006068
17	—	—	-0.00000001991
18	—	—	0

follows:

$$\frac{f_i^{n+1} - f_i^n}{\Delta\tau} + 2i\Omega_1 f_i^n = \frac{f_{i+1}^n - 2f_i^n + f_{i-1}^n}{\Delta\eta^2} + \frac{a}{\Delta\eta^2\Delta\tau}\left[\left(f_{i+1}^{n+1} - 2f_i^{n+1} + f_{i-1}^{n+1}\right) - \left(f_{i+1}^{n-1} - 2f_i^{n-1} + f_{i-1}^{n-1}\right)\right] + \frac{b}{\Delta\eta^4}\left(f_{i+1}^n - 2f_i^n + f_{i-1}^n\right)\left(f_{i+1}^n + f_{i-1}^n\right)\left(\bar{f}_{i+1}^n + \bar{f}_{i-1}^n\right) + \frac{b}{2\Delta\eta^4}\left(f_{i+1}^n + f_{i-1}^n\right)^2\left(\bar{f}_{i+1}^n - 2\bar{f}_i^n + \bar{f}_{i-1}^n\right). \tag{11}$$

The boundary condition at (9) indicated that the velocity profile tended to be zero while the length tended to be infinite. The finite difference method has converted the infinite problem from $[0, \infty)$ to finite problem [10, 11]. In the hybrid finite difference–asymptotic interpolation method, the problem is explored with 3 or more distinct unit lengths such as $L = 6,12,18$, and the results of velocity profiles are shown in Tables 1 and 2. Table 1 presents the real part of fluid's velocity. Meanwhile, Table 2 presents the imaginary part of fluid's velocity. The data illustrates that the velocity for each length are different.

Although the results are converging, the velocity profile began to slightly show a difference at $\eta \geq 2$. Therefore, an asymptotic interpolation method is added to the system using a special function of $y = a_1 + a_2 e^{-a_3^2 L}$ [26–28].

The hybrid approach used the idea of the least square nonlinear to determine the best fit for each node. Table 3 shows the velocity profile after using the hybrid method. The results fulfill the condition in (9) where the fluid's velocity decreases as length increase. The validation of the hybrid method can be seen in [28].

Table 3: Velocity profile via hybrid method.

η	Real part, u	Imaginary part, v
0	1.0000	0.0000
1	0.3449	-0.0332
2	0.1164	-0.0225
3	0.0393	-0.0114
4	0.0134	-0.0052
5	0.0046	-0.0022
6	0.0010	-0.0009

2.3. Error Analysis. The theory of perturbation is applied to evaluate the error of the numerical system. Assumed that the system has $Af^* = b + \delta b$ with $f^* = f + \delta f$, where δb and δf are perturbation of b and f, the truncation error in (8) is highlighted. When the truncation error is moved to the right side, the perturbation of b can be described as

$$\delta b \approx \frac{(u+iv)_{\tau\tau}\Delta\tau}{2} + \frac{(u+iv)_{\eta\eta\eta\eta}\Delta\eta^2}{24} + \frac{\left[(u+iv)_{\tau}\right]_{\eta\eta\eta\eta}\Delta\eta^2}{24} + \frac{\left[(u+iv)_{\eta\eta}\right]_{\tau\tau\tau}\Delta\tau^2}{6} + \frac{(u+iv)_{\eta\eta}(u+iv)_{\eta}(u-iv)_{\eta\eta\eta}\Delta\eta^2}{6} + \frac{\left[(u+iv)_{\eta}\right]^2(u+iv)_{\eta\eta\eta\eta}\Delta\eta^2}{24}. \tag{12}$$

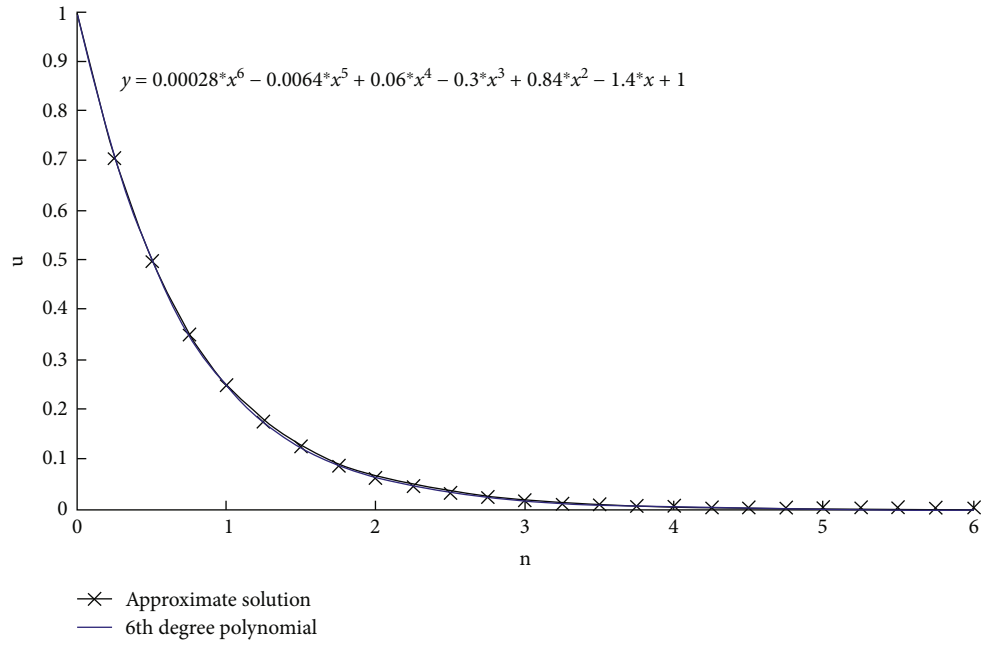

Figure 2: Sixth-degree polynomial fit with real part of velocity profile.

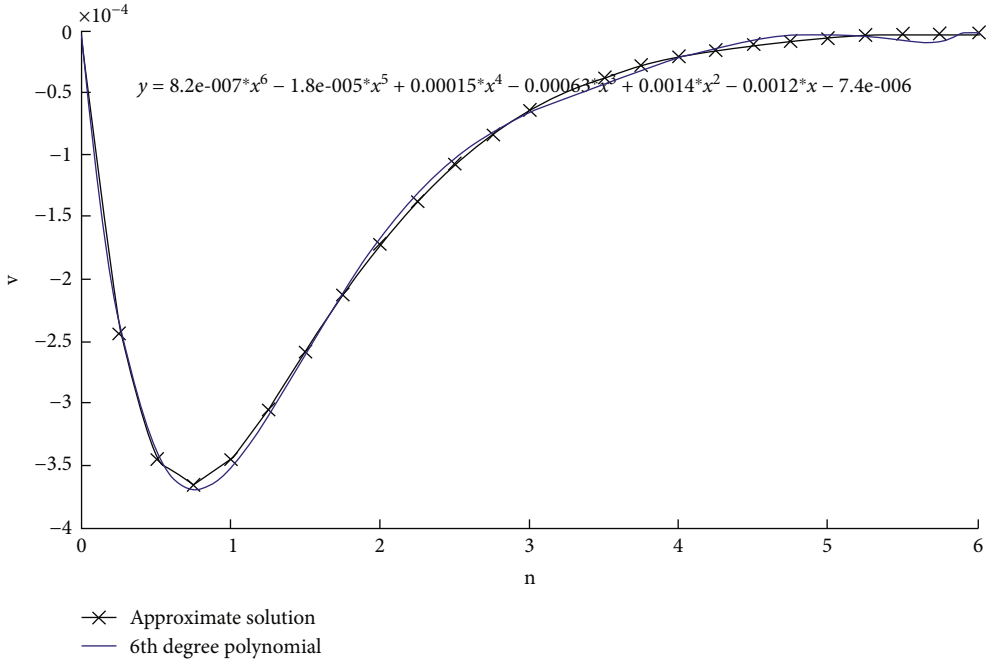

Figure 3: Sixth-degree polynomial fit with imaginary part of velocity profile.

In this paper, error analysis is carried out using two methods: (1) 6th degree of polynomial curve fit and (2) modified problem with an exact solution.

Figures 2 and 3 demonstrate the 6th degree of polynomial function for the real part and the imaginary part of the velocity profile.

Step sizes are chosen to be $\Delta\eta = 1/4$ and $\Delta\tau = 1/1000$, where the time step is too small $\Delta\tau \ll \Delta\eta$. Thus, (12) is reduced by ignoring higher order of $\Delta\tau$.

$$\delta b \approx \frac{(u+iv)_{\eta\eta\eta\eta}\Delta\eta^2}{24} + \frac{(u+iv)_{\eta\eta}(u+iv)_{\eta}(u-iv)_{\eta\eta\eta}\Delta\eta^2}{6} + \frac{\left((u+iv)_{\eta}\right)^2(u+iv)_{\eta\eta\eta\eta}\Delta\eta^2}{24}. \tag{13}$$

Let $u_1 = u_{\eta\eta\eta\eta}\Delta\eta^2/24$, $u_2 = u_{\eta\eta}u_\eta u_{\eta\eta\eta}\Delta\eta^2/6$, and $u_3 = (u_\eta)^2 u_{\eta\eta\eta\eta}\Delta\eta^2/24$. The derivatives of the polynomial function shown in Figure 1 are considered. The condition of the norm and inequality of $\|u_1 + u_2 + u_3\| \le \|u_1\| + \|u_2\| + \|u_3\|$ are satisfied, where $\|u_1 + u_2 + u_3\| = 0.1008$ and $\|u_1\| + \|u_2\| + \|u_3\| = 0.3231$. Figure 2 shows the 6th-degree polynomial fit for the imaginary part. The condition also satisfied where $\|v_1 + v_2 + v_3\| = 0.2755$ and $\|v_1\| + \|v_2\| + \|v_3\| = 0.3159$. These numbers confirmed that the truncation error of the finite difference method is adequate.

The implicit numerical scheme of the modified third-grade fluid is carried out with the exact solution shown in Figure 4 with $u = \tau/1 + 3\eta$ and $v = -0.001\eta\tau/e^\eta$.

Equation (8) now becomes

$$\frac{\partial f}{\partial \tau} + 2i\Omega_1 f = \frac{\partial^2 f}{\partial \eta^2} + a\frac{\partial^3 f}{\partial \eta^2 \partial \tau} + 2b\left[2\left(\frac{\partial^2 f}{\partial \eta^2}\right)\left(\frac{\partial f}{\partial \eta}\right)\left(\frac{\partial \bar{f}}{\partial \eta}\right) + \left(\frac{\partial f}{\partial \eta}\right)^2\left(\frac{\partial^2 \bar{f}}{\partial \eta^2}\right)\right] + g(\eta, \tau), \tag{14}$$

where

$$\begin{aligned} g(\eta,\tau) = {} & \frac{1}{1+3\eta} + 2i\left(\frac{\tau}{1+3\eta} - \frac{0.001i\eta\tau}{e^\tau}\right) - \frac{18\tau}{(1+3\eta)^3} \\ & - \frac{0.002i\tau}{e^\eta} + \frac{0.001i\eta\tau}{e^\eta} - \frac{18}{(1+3\eta)^3} - \frac{0.002i}{e^\eta} \\ & - 4\left(-\frac{3\tau}{(1+3\eta)^2} - \frac{0.001i\tau}{e^\eta} + \frac{0.001i\eta\tau}{e^\eta}\right)^2 \\ & \cdot \left(\frac{18\tau}{(1+3\eta)^3} + \frac{0.002i\tau}{e^\eta} - \frac{0.001i\eta\tau}{e^\eta}\right) \\ & - 2\left(-\frac{3\tau}{(1+3\eta)^2} - \frac{0.001i\tau}{e^\eta} + \frac{0.001i\eta\tau}{e^\eta}\right)^2 \\ & \cdot \left(\frac{18\tau}{(1+3\eta)^3} - \frac{0.002i\tau}{e^\eta} + \frac{0.001i\eta\tau}{e^\eta}\right). \end{aligned} \tag{15}$$

Error analysis for finite difference method is performed. Inequality of $(\|\delta b\|/\|A\|.\|A\|^{-1}\|b\|) \le (\|\delta x\|/\|x\|) \le (\|A\|.\|A\|^{-1}\|\delta b\|/\|b\|)$ is calculated in attempt to discover a relative change. Equation (13) is highlighted, and the observation is covered at τ_2. This inequality is fulfilled with the lower bound $\|\delta b\|/\|A\|.\|A\|^{-1}\|b\| = 0.0001$, relative error $\|\delta x\|/\|x\| = 0.0831$, and upper bound of $\|A\|.\|A\|^{-1}\|\delta b\|/\|b\| = 0.3870$. From this exploration, the relative error is noticeably small which is at 8.31%. It demonstrated the validity of the approximate solution by numerical approach of finite difference method for this modified fluid problem. The following figure portrays the velocity profile after the combination of the asymptotic interpolation method.

The Newton method concept has been employed in error analysis for asymptotic interpolation. The least square nonlinear equation is used to generate three nonlinear equations from a special function:

$$\begin{aligned} & \sum_{i=1}^{3} y_i - a_1 - a_2 e^{-a_3^2 x_i} = 0 = F_1, \\ & \sum_{i=1}^{3} e^{-a_3^2 x_i}\left(y_i - a_1 - a_2 e^{-a_3^2 x_i}\right) = 0 = F_2, \\ & \sum_{i=1}^{3}\left(y_i - a_1 - a_2 e^{-a_3^2 x_i}\right) a_3 x_i \left(a_2 e^{-a_3^2 x_i}\right) = 0 = F_3. \end{aligned} \tag{16}$$

The results are perturbed as $y_i + \delta y_i$, where $\delta y = \delta b$. Equation (16) then transformed to

$$\begin{aligned} & \sum_{i=1}^{3} y_i + \delta y_i - a_1^* - a_2^* e^{-a_3^{*2} x_i} = 0 = f_1, \\ & \sum_{i=1}^{3} e^{-a_3^{*2} x_i}\left(y_i + \delta y_i - a_1^* - a_2^* e^{-a_3^{*2} x_i}\right) = 0 = f_2, \\ & \sum_{i=1}^{3}\left(y_i + \delta y_i - a_1^* - a_2^* e^{-a_3^{*2} x_i}\right) \cdot a_3^* x_i \left(a_2^* e^{-a_3^{*2} x_i}\right) = 0 = f_3, \end{aligned} \tag{17}$$

where a_1^*, a_2^*, a_3^* are the coefficients at the exact solution and a_1, a_2, a_3 are the coefficient at the approximate solution. The small changes of each coefficient are $a_1^* = a_1 + \delta a_1$, $a_2^* = a_2 + \delta a_2$, and $a_3^* = a_3 + \delta a_3$. For the next step, the formulae below are considered.

$$\begin{aligned} F_1(a^*) &= \sum_{i=1}^{3} y_i - a_1^* - a_2^* e^{-a_3^{*2} x_i} = -\sum_{i=1}^{3} \delta y_i = p_1, \\ F_2(a^*) &= \sum_{i=1}^{3} e^{-a_3^{*2} x_i}\left(y_i - a_1^* - a_2^* e^{-a_3^{*2} x_i}\right) \\ &= -\sum_{i=1}^{3} e^{-a_3^{*2} x_i}\delta y_i = p_2, \\ F_3(a^*) &= \sum_{i=1}^{3}\left(y_i - a_1^* - a_2^* e^{-a_3^{*2} x_i}\right) a_3^* x_i \left(a_2^* e^{-a_3^{*2} x_i}\right) \\ &= -\sum_{i=1}^{3} a_3^* x_i \left(a_2^* e^{-a_3^{*2} x_i}\right)\delta y_i = p_3. \end{aligned} \tag{18}$$

For $p_i = 0 \longrightarrow f_i = F_i$, by considering the assumptions below, let $F(a) = 0$ be an approximate solution; meanwhile, $F(a^*) = p(a^*)$ is an exact solution, and let $a^* = a + \Delta a$. Therefore,

$$F(a^*) - F(a) = p(a^*), \tag{19}$$

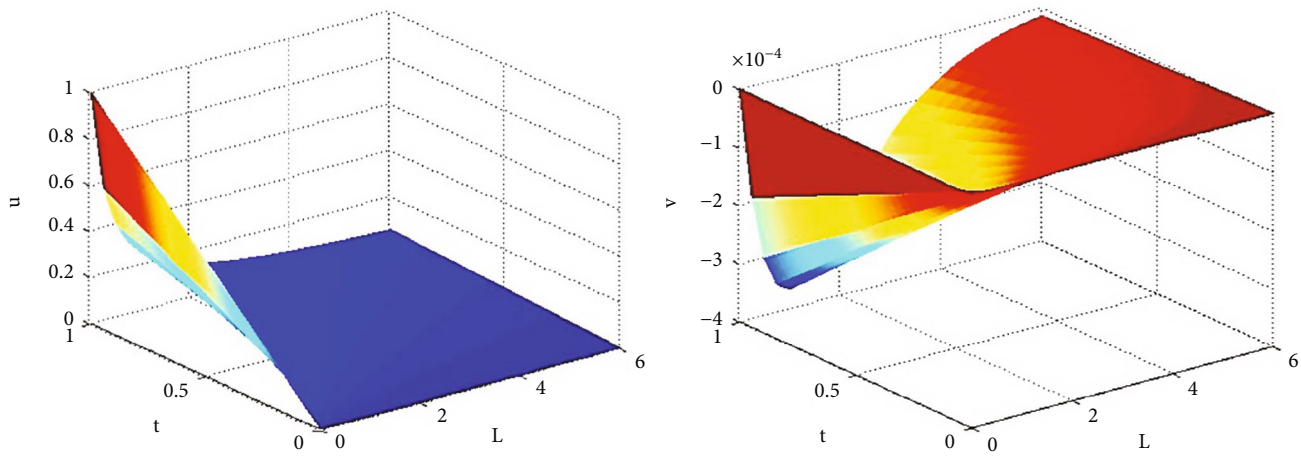

Figure 4: Exact solution.

$$F(a^*) = F(a + \Delta a) = F(a) + \Delta a F'(a) + O(\Delta a^2). \quad (20)$$

Equation (19) then changed into $\Delta a = (F'(a))^{-1} p(a + \Delta a)$. By using linearization and by assuming that Δa is very small, the equation is reduced to $[F'(a) - \mathbf{K}][\Delta a_1\ \Delta a_2\ \Delta a_3]^T = \mathbf{R}$, where $\mathbf{K}$ and $\mathbf{R}$ are a matrix with coefficient and a vector without coefficient of Δa_i. Based on the findings obtained by Mahadi et al. [26–28], the interest of this error analysis for asymptotic interpolation is Δa_1. The comparison of Δa_1 and the error of solution is shown in Table 4. This demonstrates how closely the two error calculations match up.

The norm of relative error comparison between the hybrid method and the finite difference method with respect to the exact solution is shown in Table 5.

The relative error norm of the hybrid method is smaller than that of the finite difference method. As a result, it is suggested that one of the numerical methods for improving performance when handling an infinite domain of boundary conditions is the hybrid method. The two error analyses mentioned above real-time error analysis which do not require the knowledge of exact solution. Thus, these error analysis can be used for adaptive finite difference method where the grid size can be adjusted in real time to achieve user-supplied error tolerance.

3. Results

The third-grade non-Newtonian fluid in a rotating frame is studied. A novel hybrid method that combines the finite difference method with asymptotic interpolation is intended to improve the finite difference results. This method's objective is to satisfy the boundary condition. The numerical solution is approximated using the least square nonlinear approach for a specific special function. The results are reported in Tables 1–3.

The real part of fluid velocity is shown in Table 1 for different lengths such as $L = 6$, $L = 12$, and $L = 18$. The number of data will increase as the lengths increase. The fluid has zero velocity at $L = 6$, when $\eta = 6$. In comparison to $L = 12$ and $L = 18$, the fluid has a low velocity which is not equal to zero. These data show that the fluid still have velocity even small as the problem's length increase. Table 2 displays the fluid velocity for the imaginary part of the problem as well as the same explanations. These findings demonstrate that the exact velocity can be determined after certain length iterations. Table 3 shows the fluid velocity after utilizing the hybrid technique, which incorporates length iterations and the relevant special function. These results satisfy the boundary condition in (9) as proved by the fact that at $L = 6$, the velocity tends to a low number that is not equal to zero.

Table 4: Comparison of Δa_1 and error of solution.

η	Δa_1	Error of solution
2.0	0.0841	0.0815
2.5	0.0841	0.0868
3.0	0.0840	0.0844
3.5	0.0839	0.0789
4.0	0.0835	0.0727

Table 5: Comparison of norm of relative error.

Velocity profile	Finite difference method	Hybrid method
u	2.97*E*-01	3.74*E*-02
v	2.69*E*-01	6.67*E*-03

The polynomial fit, as illustrated in Figures 2 and 3, for the real and imaginary parts, respectively, has been used to conduct error analysis. The polynomial curve fit is employed to identify the ideal graph for the finite difference process's evaluation of the truncation error. Instances where the left side's value is lower than the right side satisfy the norm and inequality requirement.

The modified problem is created, and the error analysis is performed for the finite difference method and asymptotic interpolation. The modified problem has the exact solution given in Figure 4. The results of the hybrid approach are shown in Figure 5. The relative inaccuracy found is within

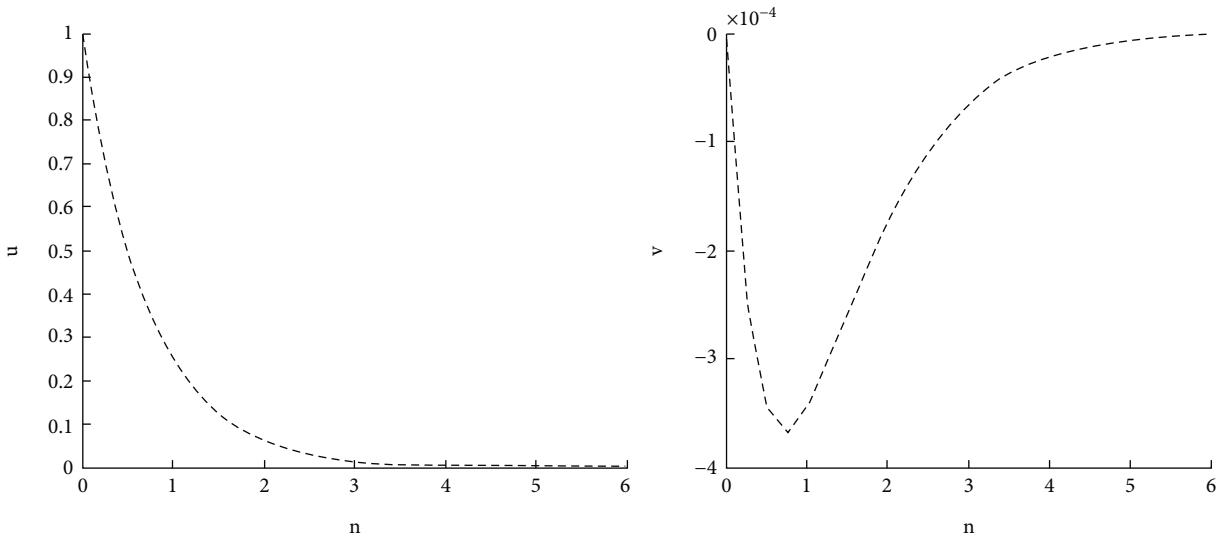

Figure 5: Approximate solution by hybrid approach.

the acceptable range. As a result, the finite difference method's output is accurate. Next, a_1 is the main focus of the error analysis for asymptotic interpolation. Table 4 demonstrates that the Δa_1 error of solution between the exact and hybrid approaches is relatively small.

The norm of relative errors between the hybrid approach and the finite difference method is shown in Table 5. It demonstrates that the hybrid method's norm of relative error is small for both the real and imaginary parts.

4. Summary and Conclusions

The paper centered on a hybrid technique for responding to a semi-infinite boundary condition for unsteady flow of a non-Newtonian third-grade fluid. The present paper examined the error of the approximate solution to ensure that the hybrid method is effective in solving the problem. There are two approaches to error analysis. First, the perturbation method is applied to the fluid problem. Truncation errors in finite difference are investigated, as well as the 6^{th} degree of polynomial functions. Second, the exact solution to a modified fluid problem is identified. The exact solution, as well as the results of the finite difference method, the hybrid finite difference method, and asymptotic interpolation method, is presented. The findings of this investigation indicate the following:

(i) The hybrid approach has a low relative error norm

(ii) It suggests that for an indefinite problem, the hybrid method could produce accurate solutions

(iii) These real-time error analysis techniques can be used to design an adjustable mesh size finite difference approach with user-supplied error tolerance

The problem of non-Newtonian fluid flow has been addressed using the hybrid finite difference–asymptotic interpolation method. This method is useful for complicated geometry problem in real-time simulation with infinite domain.

Data Availability

The paper contains all relevant data.

Conflicts of Interest

The authors declare that there is no conflict of interests regarding the publication of the paper.

Acknowledgments

The authors would like to express their gratitude to Universiti Teknologi MARA Cawangan Johor for funding this research under Geran Penyelidikan Bestari Vot No. 29000. The authors are also appreciative to the reviewers for attentively reading this article and providing helpful comments and suggestions.

References

[1] R. Seshagiri, G. Vinod, and A. Alexander, "Bullet proof vest using non-Newtonian fluid," *International Journal of Students' Research in Technology Management*, vol. 3, no. 8, pp. 451–454, 2015.

[2] W. Xiu, S. Wang, W. Qi, X. Li, and C. Wang, "Disaster chain analysis of landfill landslide: scenario simulation and chain-cutting modeling," *Sustainability*, vol. 13, no. 9, p. 5032, 2021.

[3] T. Gul, S. Miraj-ul-Haq, Z. Shah, and M. A. Khan, "Unsteady second grade plug flow between two vertical oscillating plates under the effect of (MHD) and temperature," *Journal of Applied Environmental and Biological Sciences*, vol. 5, no. 7, pp. 279–289, 2015.

[4] I. Khan, F. Ali, N. Mustapha, and S. Shafie, "Closed-form solutions for accelerated MHD flow of a generalized burgers' fluid

in a rotating frame and porous medium," *Boundary Value Problems*, vol. 2015, p. 8, 2015.

[5] K. Khandelwal and V. Mathur, "Exact solutions for an unsteady flow of viscoelastic fluid in cylindrical domains using the fractional Maxwell model," *International Journal of Applied and Computational Mathematics*, vol. 1, no. 1, pp. 143–156, 2015.

[6] M. Parida and S. Padhy, "Numerical study of MHD flow of a third grade fluid in a non-Darcian porous channel," *International Journal of Pure and Applied Mathematics*, vol. 118, no. 3, pp. 651–665, 2018.

[7] I. K. Zeeshan, N. Amina, and N. H. Alshammari, "Double-layer coating using MHD flow of third-grade fluid with hall current and heat source/sink," *Physics*, vol. 19, no. 1, pp. 683–692, 2021.

[8] M. Khan, S. Zuhra, R. Nawaz et al., "Numerical analysis of bioconvection-MHD flow of Williamson nanofluid with gyrotactic microbes and thermal radiation: new iterative method," *Physics*, vol. 20, no. 1, pp. 470–483, 2022.

[9] T. Hayat, R. Ellahi, and F. Mahomed, "The analytical solutions for magnetohydrodynamic flow of a third order fluid in a porous medium," *Zeitschrift f¨ur Naturforschung A*, vol. 64, no. 9-10, pp. 531–539, 2009.

[10] S. Abelman, E. Momoniat, and T. Hayat, "Steady MHD flow of a third grade fluid in a rotating frame and porous space," *Nonlinear Analysis: Real World Applications*, vol. 10, no. 6, pp. 3322–3328, 2009.

[11] T. Hayat and Y. Wang, "Magnetohydrodynamic flow due to noncoaxial rotations of a porous disk and a fourth-grade fluid at infinity," *Mathematical Problems in Engineering*, vol. 2003, Article ID 674518, 18 pages, 2003.

[12] M. Nazari, *Approximate Analytical Solutions for Viscoelastic Differential Type Flow Models Using Homotopy Analysis Method, [Ph.D. thesis]*, Universiti Teknologi Malaysia, 2014.

[13] G. Van and A. Robert, "Optimal homotopy analysis and control of error for implicitly defined fully nonlinear differential equations," *Numerical Algorithms*, vol. 81, no. 1, pp. 181–196, 2019.

[14] F. Ghani, T. Gul, S. Islam et al., "Unsteady MHD thin film flow of a third grade fluid over an oscillating inclined belt embedded in a porous medium," *Thermal Science*, vol. 2015, p. 54, 2015.

[15] R. Bordoloi and N. Ahmed, "MHD free convection from a semi-infinite vertical porous plate with diffusion-thermo effect," *Biointerface Research in Applied Chemistry*, vol. 12, no. 6, pp. 7685–7696, 2021.

[16] M. Şenol, İ. Timuçin Dolapçı, Y. Aksoy, and M. Pakdemirli, "Perturbation-iteration method for first-order differential equations and systems," *Abstract and applied analysis*, vol. 2013, Article ID 704137, 6 pages, 2013.

[17] A. Mohamad, I. Khan, L. Jiann, S. Shafie, Z. Mat Isa, and Z. Ismail, "Heat transfer on rotating second grade fluid through an accelerated plate," *Malaysian Journal of Fundamental and Applied Sciences*, vol. 13, no. 3, pp. 219–223, 2017.

[18] N. Rawi, N. Zin, A. Khalid, A. Kasim, Z. Isa, and S. Shafie, "Numerical solutions for convective boundary layer flow of micropolar Jeffrey fluid with prescribe wall temperature," *Journal of the Indonesian Mathematical Society*, vol. 26, no. 3, pp. 286–298, 2020.

[19] S. Gaffar, V. Prasad, P. Reddy, and B. Khan, "Radiative flow of third grade non-Newtonian fluid from a horizontal circular cylinder," *Nonlinear Engineering*, vol. 8, no. 1, pp. 673–687, 2019.

[20] F. Al-Shibani, A. Ismail, and F. Abdullah, "The implicit Keller box method for the one dimensional time fractional diffusion equation," *Journal of Applied Mathematics and Bioinformatics*, vol. 2, no. 3, p. 69, 2012.

[21] M. Rahman, M. Ferdows, M. Shamshuddin, A. Koulali, and M. R. Eid, "Aiding (opponent) flow of hybrid copper-aluminum oxide nanofluid towards an exponentially extending (lessening) sheet with thermal radiation and heat source (sink) impact," *Journal of Petroleum Science and Engineering*, vol. 215, article 110649, 2022.

[22] B. S. Goud, Y. D. Reddy, S. Mishra, M. I. Khan, K. Guedri, and A. M. Galal, "Thermal radiation impact on magneto-hydrodynamic heat transfer micropolar fluid flow over a vertical moving porous plate: a finite difference approach," *Journal of the Indian Chemical Society*, vol. 99, no. 8, article 100618, 2022.

[23] I. Nayak, "Numerical study of MHD flow and heat transfer of an unsteady third grade fluid with viscous dissipation," *IAENG International Journal of Applied Mathematics*, vol. 49, no. 2, pp. 1–8, 2019.

[24] S. Cengizci, "An asymptotic-numerical hybrid method for solving singularly perturbed linear delay differential equations," *International Journal of Differential Equations*, vol. 2017, Article ID 7269450, 8 pages, 2017.

[25] Z. Aziz, M. Nazari, F. Salah, and D. Ching, "Constant accelerated flow for a third-grade fluid in a porous medium and a rotating frame with the homotopy analysis method," *Mathematical Problems in Engineering*, vol. 2012, Article ID 601917, 14 pages, 2012.

[26] S. Mahadi, Z. Aziz, Y. Hoe, F. Salah, and F. Nasrudin, "Numerical solution of hybrid method for third grade flow due to variable accelerated plate in a rotating frame," *Engineering and Technology*, vol. 7, no. 2.15, pp. 98–101, 2018.

[27] S. Mahadi, F. Salah, N. Arbin, and S. Yeak, "Hybrid numerical solution for unsteady state of constant accelerated MHD in a third-grade fluid with a rotation," *Journal of Physics: Conference Series*, vol. 1489, no. 1, article 012007, 2020.

[28] S. Mahadi, Y. Hoe, N. Arbin, and F. Salah, "Numerical solution for unsteady acceleration MHD third-grade fluid flow in a rotating frame through porous medium over semi-infinite boundary condition with a presence of heat transfer," *Journal of Advanced Research in Fluid Mechanics and Thermal Sciences*, vol. 87, no. 2, pp. 90–105, 2021.

[29] A. Abbas, M. Jeelani, and N. Alharthi, "Magnetohydrodynamic effects on third-grade fluid flow and heat transfer with Darcy–Forchheimer law over an inclined exponentially stretching sheet embedded in a porous medium," *Magnetochemistry*, vol. 8, no. 6, p. 61, 2022.

[30] T. Hayat, R. Naz, and S. Abbasbandy, "Poiseuille flow of a third grade fluid in a porous medium," *Transport in Porous Media*, vol. 87, no. 2, pp. 355–366, 2011.